Original Research

Changes in gene expression and neuroinflammation in the hippocampus of rats with poststroke cognitive impairment

Jiemei Chen*, Jiena Hong*, Chao Li, Yan Zeng, Mengshu Xie, Xue Zhang and Hongmei Wen

Department of Rehabilitation Medicine, The Third Affiliated Hospital, Sun Yat-Sen University, Guangzhou 510630, Guangdong Province, China
*These authors contributed equally to this paper.
Corresponding author: Hongmei Wen. Email: wenhongm@mail.sysu.edu.cn

Impact Statement

Activation of neuroinflammation and long-term changes in gene expression patterns in the hippocampus could be essential in the development of poststroke cognitive impairment (PSCI). This study indicates an important role of neuroinflammation in the development of PSCI and changes in the expression of regulatory genes in the hippocampus. The results showed that microglial activation and white matter damage were maintained in rats with PSCI during the recovery stage of cerebral ischemia. The mechanism may be related to the regulation of steroid biosynthesis and intestinal immunity and to potential key genes such as Acta2, Calb2, and Cxcl12 in the hippocampus. This study may provide new insight into the pathogenesis and treatment of PSCI.

Abstract

Poststroke cognitive impairment (PSCI) often occurs during the stroke recovery period and greatly increases the difficulty of rehabilitation. Activation of neuroinflammation and long-term changes in gene expression patterns in the hippocampus could be essential in the development of PSCI. Therefore, this study aimed to identify neuroinflammation and changes in gene expression patterns in the hippocampus in rats with PSCI. Rats underwent transient middle cerebral artery occlusion (tMCAO) or sham surgery. The infarct volume was measured on day 3 after surgery. The Morris water maze (MWM) test was used to assess cognitive function. Microglial activation and white matter (WM) lesions in the hippocampus were evaluated on day 28 after surgery. In addition, we compared differentially expressed genes (DEGs) in the hippocampus between tMCAO group rats and sham group rats by RNA sequencing. Then, Gene Ontology (GO), Kyoto Encyclopedia of Genes and Genomes (KEGG), and protein–protein interaction (PPI) network analyses were conducted to investigate these DEGs. The results showed that the tMCAO group rats showed extensive infarction and cognitive dysfunction compared with the sham group rats. Microglial activation and WM damage were obvious in the hippocampus of tMCAO group rats. We found 43 DEGs by RNA sequencing: 29 genes with upregulated expression and 14 genes with downregulated expression. The GO analysis indicated that DEGs were mainly involved in cell proliferation and differentiation, cholesterol synthesis, and metabolism. The KEGG pathway analysis suggested that the DEGs were significantly enriched in intestinal immune network for IgA production and steroid biosynthesis. Acta2, Calb2, and Cxcl12 were notable in the PPI analysis. Our results suggest that microglial activation and WM damage are maintained in rats with PSCI. The mechanism may be related to the regulation of steroid biosynthesis, intestinal immunity, and potential key genes such as Acta2, Calb2, and Cxcl12 in the hippocampus.

Keywords: Stroke, cognitive impairment, hippocampus, microglia, white matter, RNA sequencing

***Experimental Biology and Medicine* 2023; 248: 883–896. DOI: 10.1177/15353702231157922**

Introduction

Stroke has a high incidence, a high fatality rate, and a high disability rate worldwide.[1] Stroke can cause serious deficits in motor and cognitive functions and results in a major economic burden on society. Poststroke cognitive impairment (PSCI) is a subtype of vascular cognitive impairment and has a substantial impact on the functional recovery of stroke patients, profoundly affecting their health and quality of life. The prevalence of PSCI in ischemic stroke patients ranges from 25% to 70%; it tends to increase gradually over time due to developments in modern medicine and is accompanied by increasing survival rates in stroke patients.[2]

Although PSCI involves vascular risk factors, hypertension, diabetes, atrial fibrillation, cerebral artery stenosis, microglial activation, and β amyloid deposition, the underlying molecular mechanisms remain unclear.[3–6] In addition, there is currently no effective treatment, which greatly increases the difficulty of rehabilitation and inevitably imposes heavy burdens related to clinical care and medical expenses.[7,8] Thus, an improved understanding of the pathogenesis of PSCI is crucial for the development of various

neurobiological therapeutic strategies to prevent PSCI and improve the treatment effect.

The hippocampus is one of the best-studied structures in the brain and has been proven to play a very important role in cognitive functions.[9] Secondary (delayed) poststroke damage, including activation of neuroinflammation and white matter (WM) damage in the hippocampus, could be essential in the development of PSCI. The molecular mechanisms could involve long-term changes in gene expression patterns. The identification of changes in gene expression patterns is a necessary step toward understanding the development of PSCI.[10] Therefore, this study aimed to identify whether cognitive dysfunction, activation of neuroinflammation, and WM damage are present during the recovery stage in rats subjected to transient middle cerebral artery occlusion (tMCAO). Furthermore, RNA sequencing and bioinformatic analyses were performed to elucidate differential gene expression profiles and gene functions in the hippocampus.

Materials and methods

Animals

The study was approved by the Animal Care Committee of South China Agricultural University (Guangzhou, China) and was conducted in accordance with the Guidelines of the Care and Use of Laboratory Animals issued by the Chinese Council on Animal Research. Seven-week-old male Sprague-Dawley (SD) rats (230–250 g) were purchased from Guangdong Medical Laboratory Animal Center (Guangzhou, China). A total of 50 rats were used in this study, and they were raised in a specific pathogen-free (SPF) unit on a 12-h light/dark cycle at an ambient temperature of 21 ± 1°C and ambient humidity of 50 ± 5%. All efforts were made to minimize the pain and stress of the rats.

tMCAO model and experimental grouping

After deep anaesthetization by intraperitoneal injection of pentobarbital, 32 SD rats were randomly selected and subjected to left tMCAO for 90 min as described in previous studies.[11,12] Briefly, the left common carotid artery (CCA), external carotid artery (ECA), and internal carotid artery (ICA) were exposed through a midline neck incision. Next, the CCA and ECA were separated upward and ligated, and the ICA was occluded by placement of a temporary atraumatic clip. Then, a loose suture was placed around the CCA, and a monofilament (Rui Wo De, Shenzhen, China) was inserted into the CCA through a cut made with sharp scissors proximal to the CCA ligature 5 mm from the bifurcation of the ECA and ICA. The suture around the CCA was tightened, and the clip was then removed from the ICA. The monofilament was slowly advanced further into the ICA to the origin of the middle cerebral artery (MCA) until resistance was felt, which indicated occlusion of the MCA. The rats were returned to their cages, and the monofilaments remained in place for 90 min until withdrawal to allow reperfusion. Poststroke neurological deficits were graded according to the Bederson scale[13,14] after the rats regained full consciousness. Neurological function was scored on a scale of 0–5: 0, no neurological deficits; 1, inability to fully extend the right forepaw; 2, leaning to the right; 3, falling to the right; 4, lack of self-awareness and a low level of consciousness; and 5, death. tMCAO rats with scores of 1–3 were enrolled as the tMCAO group ($n = 18$). In addition, 18 SD rats were subjected to the same protocol without monofilament insertion. The rats subjected to this sham operation were enrolled as the sham group ($n = 18$). The experimental schedule is presented in Figure 1(a).

Infarct volume measurement

Infarct volume was assessed by 2,3,5-triphenyltetrazolium chloride (TTC) (Sigma, St. Louis, MO, USA) staining on day 3 after surgery as described in a previous study.[15] Six rats in each group were euthanized by a pentobarbital overdose and decapitation, and the brains were removed and sliced into five coronal sections (2 mm thick) after washing in ice-cold phosphate-buffered saline. The sections were placed in a culture dish containing 2% TTC for 20 min at 37°C in the dark. The tissue was then fixed overnight in 4% formaldehyde and photographed with a camera. Infarct areas were measured with Image-Pro Plus 6.0 (Media Cybernetics, Bethesda, MD, USA). Infarct volume (%) was calculated as follows: infarct volume (%) = ((area of the contralateral hemisphere − area of the normal tissue in the ipsilateral hemisphere)/area of the contralateral hemisphere) × 100%.

Cognitive function assessment

The Morris water maze (MWM) test was used to evaluate spatial learning and memory from day 23 to day 28 after surgery. This test was carried out in a 150-cm diameter circular tank filled with water to a depth of 35 cm. The water temperature was maintained at 22 ± 2°C. An "escape platform" with a diameter of 15 cm was placed approximately 2 cm below the water surface in target quadrant III of the pool. The experiment consists of two parts: positioning navigation and space exploration. The positioning navigation test was performed on five consecutive days. On the first day, rats were placed in the water facing the wall once in each of the four quadrants. They were allowed to search for the platform for 60 s, and the time taken to locate the escape platform was recorded. The space exploration test was conducted on the sixth day, with the platform removed. The time taken for the rats to cross the platform area was recorded, as was the time that they remained in the target quadrant.

Immunofluorescence staining

After the MWM test, rats were deeply anesthetized with pentobarbital and perfused transcardially first with 0.9% saline and then with 4% paraformaldehyde in phosphate buffer. After perfusion, the brains were removed and post-fixed in 4% paraformaldehyde at 4°C for 24 h. Subsequently, the brains were dehydrated in 20% and 30% sucrose, embedded in optimal cutting temperature (OCT) compound, and sliced into 10-μm-thick sections in the coronal plane with a cryostat microtome (CM1900; Leica, Wetzlar, Germany).

Immunofluorescence staining was performed as follows: All sections were fixed with 4% paraformaldehyde for

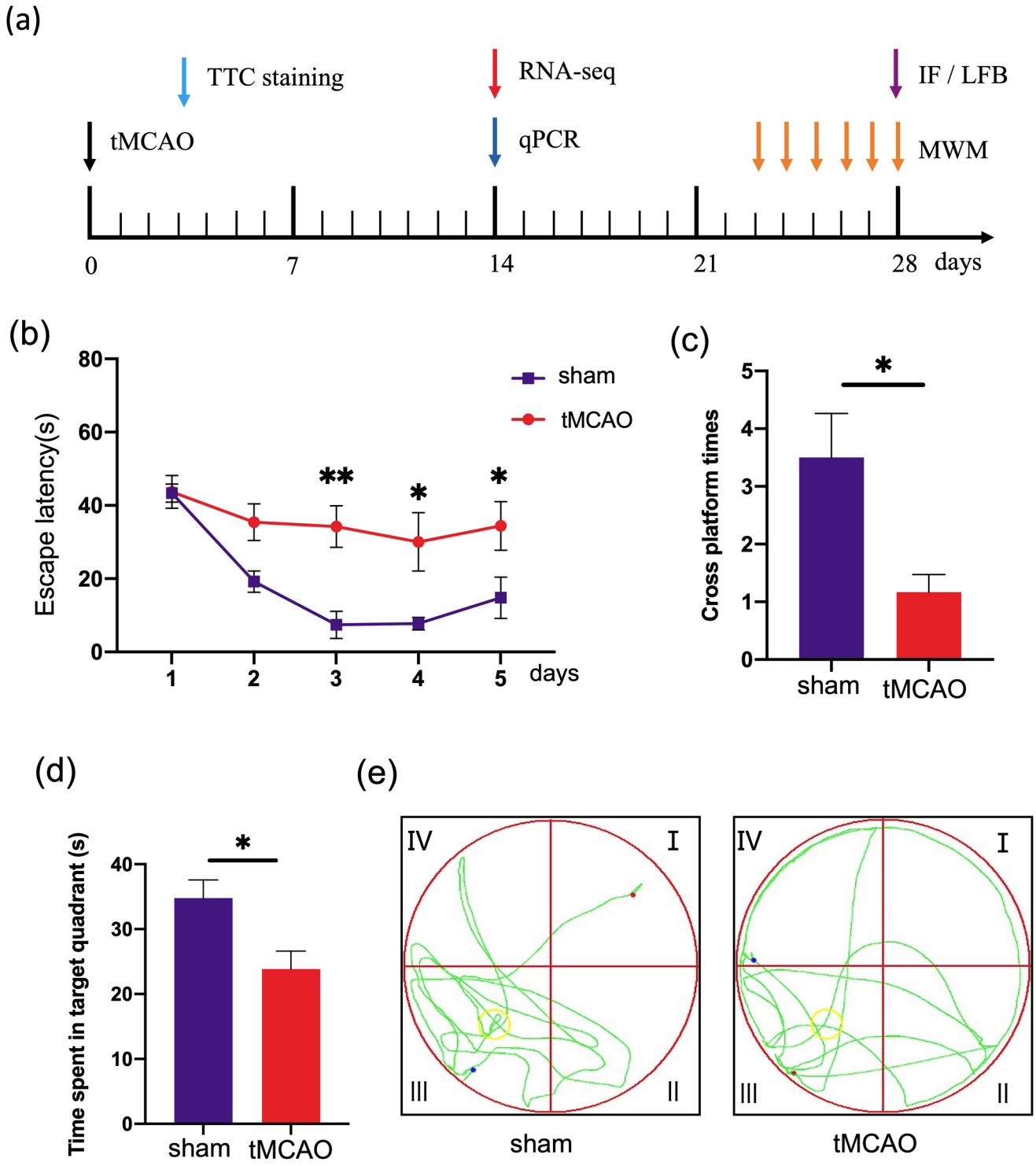

Figure 1. Experimental schedule and spatial cognitive function between the two groups. (a) Experimental schedule: different colored arrows represent experiments at different time points. (b) Average escape latency. (c) Platform crossing times. (d) Times spent in the target quadrant. (e) Representative swimming paths of the rats in the sham and tMCAO groups. The pool was divided into four quadrants: I, II, III and IV. tMCAO: transient middle cerebral artery occlusion; TTC: 2,3,5-triphenyltetrazolium chloride; RNA-seq: RNA sequencing; qPCR: quantitative polymerase chain reaction; MWM: Morris water maze; IF: immunofluorescence; LFB: Luxol fast blue. Red circles represent the water tank, yellow circles represent the platform, and green lines represent swimming paths.
*$P < 0.05$, **$P < 0.01$.

10 min at room temperature and blocked with 10% bovine serum albumin (BSA) for 1 h. Next, the sections were incubated with a rabbit anti-Iba-1 antibody (1:200; Wako, Japan) overnight at 4°C. The following day, sections were incubated with a secondary antibody at room temperature for 1 h. After rinsing, the sections were mounted with a DAPI-containing antifade solution. Fluorescence signals were then observed under a fluorescence microscope (Nikon, Tokyo, Japan).

Image-Pro Plus 6.0 (Media Cybernetics Inc., Bethesda, MD, USA) was used to evaluate the number and per-brain volume of Iba-1-positive cells.

WM lesion assessment

Luxol fast blue (LFB) staining was used to observe WM lesions as described in a previous study.[16] Frozen sections were immersed in a 1:1 alcohol:chloroform mixture for 24 h and then rehydrated with 95% ethyl alcohol. The sections were incubated in LFB (Goodbio Technology Co., Ltd., Wuhan, China) at 60°C overnight and rinsed sequentially with 95% ethanol and double distilled water. Then, the sections were placed in a lithium carbonate solution and differentiated with 70% ethanol and double distilled water for 10 s. The sections were then washed with 100% alcohol and xylene, fixed with neutral balsam, and finally observed under a microscope camera. As described in the previous reports,[17,18] the severity of WM lesions was graded as 0 (normal), 1 (disarrangement of nerve fibers), 2 (formation of marked vacuoles), and 3 (disappearance of myelinated fibers).

RNA sequencing analysis

Three rats in each group were euthanized by a pentobarbital overdose and decapitation, and the brains were carefully removed for separation of the hippocampus. Total RNA was extracted from the hippocampi of three sham-operated rats and three tMCAO rats on day 14 after surgical intervention using TRIzol reagent (Invitrogen, Carlsbad, CA, USA) in accordance with the manufacturer's instructions. The concentrations of the total RNA samples were assessed with a NanoDrop ND-1000 spectrophotometer (Thermo Fisher Scientific, Waltham, MA, USA) and confirmed by agarose gel electrophoresis. Samples with a 28S/18S RNA ratio of 1.5:2 and a 260 nm/280 nm absorbance ratio of 1.7: 2.1 were further processed. RNA sequencing libraries were generated using Illumina kits. The libraries were then subjected to quality assessment and quantified by quantitative polymerase chain reaction (qPCR). The data for each gene were normalized by calculating the fragments per kilobase per million mapped reads (FPKM) value.

Bioinformatic analyses

Gene Ontology (GO) and Kyoto Encyclopedia of Genes and Genomes (KEGG) analyses were performed using the Gene Ontology Consortium Database (http://www.geneontology.org) and the KEGG database (http://www.genome.jp/kegg). A false discovery rate (FDR)-adjusted P value <0.05 was defined as significant. Protein–protein interaction (PPI) network analysis of the proteins encoded by the differentially expressed genes (DEGs) was conducted using the Search Tool for the Retrieval of Interacting Genes (STRING) database (http://string-db.org). The PPI enrichment P value threshold was <0.01.

qPCR analysis

Three rats in each group were euthanized by a pentobarbital overdose and decapitation, and the brains were carefully removed for separation of the hippocampus. Total RNA was extracted from the hippocampal tissue of three sham-operated rats and three tMCAO rats on day 14 after surgical intervention using TRIzol reagent. Messenger RNA (mRNA) was reverse-transcribed into complementary DNA (cDNA), and qPCR was performed using a SYBR Green Master Mix Kit in accordance with the manufacturer's instructions. The glyceraldehyde-3-phosphate dehydrogenase (GAPDH) gene was used as the internal reference, and the primer sequences are shown in Table 1. Relative gene expression levels were calculated by the $2^{-\Delta\Delta Ct}$ method and normalized to GAPDH gene expression. The results are expressed as the expression ratio of the gene of interest to GAPDH.

Statistical analysis

Data are presented as mean ± SEM values. The results from the behavioral study were statistically analyzed using repeated-measures analysis of variance (ANOVA). qPCR results were analyzed using one-way ANOVA followed by Tukey's multiple comparison test. Significance was set at $P < 0.05$.

Results

Extensive infarction and cognitive dysfunction in tMCAO rats

Successful establishment of tMCAO was confirmed by TTC staining on day 3 after surgery. Rats in the sham group showed no infarction, while extensive infarction was observed in rats in the tMCAO group, as indicated in Figure 2(a).

The MWM test was performed to evaluate cognitive function after surgery. Rats in the tMCAO group exhibited an impaired learning capacity, as indicated by the increased escape latency compared with that of rats in the sham group

Table 1. The primers used in qPCR.

Gene name	Forward primer (5′-3′)	Reverse primer (5′-3′)	Amplicon size (bp)
GAPDH (rat)	GCTCTCTGCTCCTCCCTGTTCTA	TGGTAACCAGGCGTCCGATA	124
Hrct1	CGTCTCCCAAGAGTCGTTC	CCAGTATCCTCATCCATCCC	253
Il15	GTTTCCTTCTCAACAGTCACTTCTT	TCAATTTTCTCCAGATCGTATCTTA	130
Acta2	CCTGAAGTATCCGATAGAACACG	CATCTCCAGAGTCCAGCACAA	275
Calb2	CCGTCCCTATGATGAACCTAA	TAGCCGCTTCCATCCTTGT	210
Cbln4	GTTCGGAGCACCAACCAC	CAAAGACGGATTCCAGTGTG	112
Moap1	GGTGGCGGTCTCCTACCAT	GAGGGCGTCTGACCTTTGC	117

qPCR: quantitative polymerase chain reaction; Il15: interleukin 15.

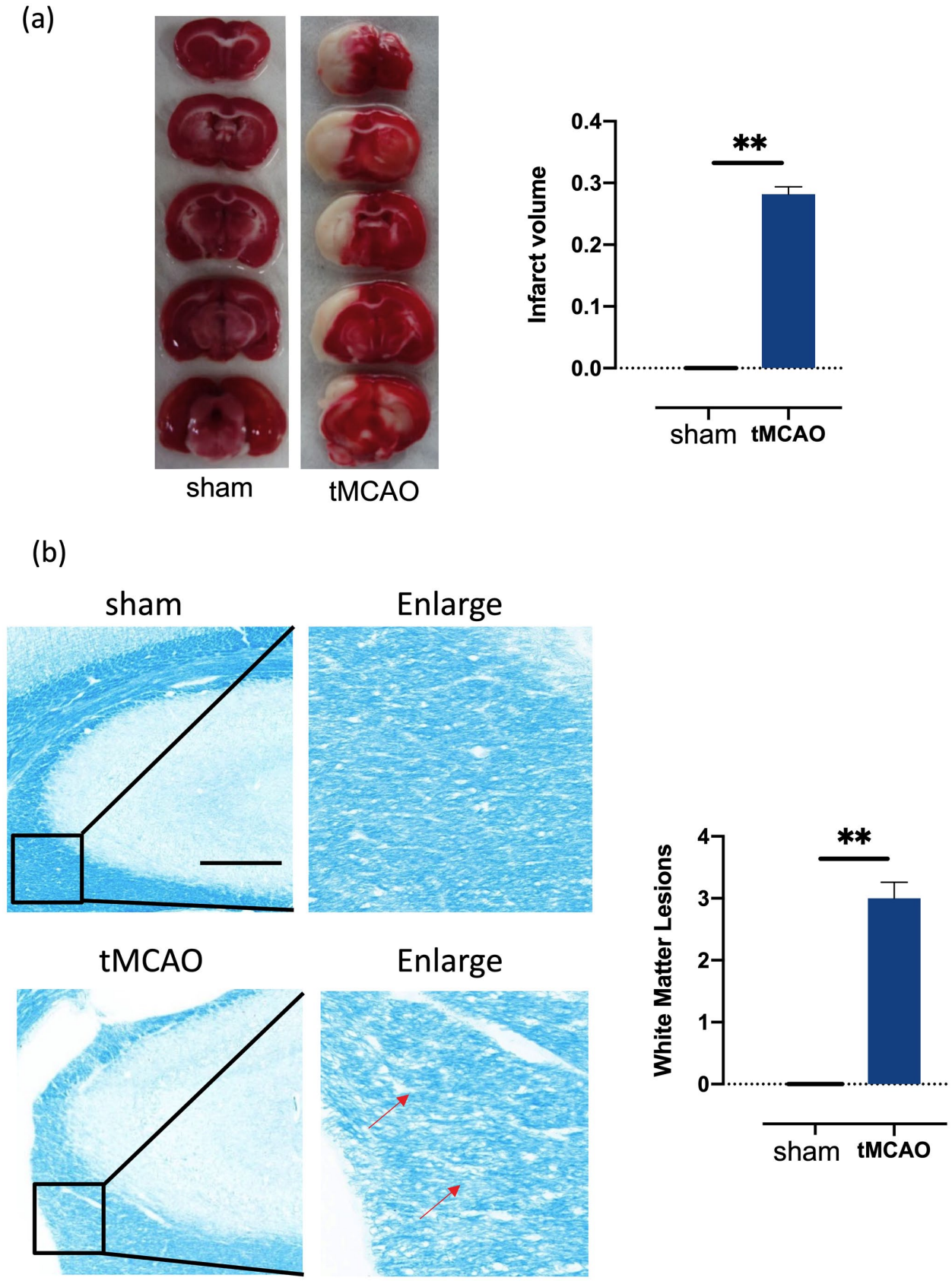

Figure 2. Comparison of infarct volume and WM damage. (a) Representative TTC-stained brain slices and comparison of infarct volume between the tMCAO and sham groups. (b) Representative images of LFB staining in the hippocampus and WM grading score histograms for each group. WM: white matter; TTC: 2,3,5-triphenyltetrazolium chloride; LFB: Luxol fast blue; tMCAO: transient middle cerebral artery occlusion.
Typical white matter lesions (disarrangement of nerve fibers) are indicated by red arrows. Bar = 500 μm.
$^{**}P < 0.01$.

on days 3, 4, and 5 after surgery (Figure 1(b)). In the space exploration test, the times taken to cross the platform (Figure 1(c)) and the times spent in the target quadrant (Figure 1(d)) were lower in the tMCAO group than in the sham group. The representative swimming paths of the two groups are presented in Figure 1(e).

WM damage and microglia activation in the hippocampus of tMCAO rats

To evaluate remyelination after stroke, we performed LFB staining on the hippocampus of rats on day 28 after surgery. Obvious WM lesions appeared in the tMCAO group compared with the sham group (Figure 2(b)).

To explore neuroinflammation in the hippocampus, activation of microglia (Iba-1-positive cells) was evaluated by immunofluorescence analysis. As shown in Figure 3(a) and (b), the microglia in the CA1 and CA3 regions and the dentate gyrus (DG) were activated in the tMCAO group compared with the sham group.

DEGs in the hippocampus

To better understand the genetic mechanisms involved, we performed RNA sequencing on hippocampi from rats in the tMCAO group and the sham group. A total of 14,586 corresponding genes were identified between the two groups: 8288 genes with upregulated expression and 6298 genes with downregulated expression. Forty-three DEGs (29 genes with upregulated expression and 14 genes with downregulated expression) exhibited significant differential expression according to two criteria: a fold change in the expression level of at least 1.5 and a P value of <0.05. A volcano plot was generated to show the DEGs based on fold changes in expression and P values (Figure 4). The top 10 upregulated and downregulated DEGs are summarized in Table 2.

GO and KEGG enrichment analyses of DEGs

GO terms were assessed to clarify the biological functions of the DEGs. The GO terms pertained to three categories: biological process (BP), cellular component (CC), and molecular function (MF). The upregulated and downregulated DEGs in the BP, CC, and MF categories are presented in Figure 5. The upregulated DEGs were enriched mainly in the BP terms epithelial cell development and differentiation, T-cell proliferation, glomerulus, blood vessel, and connective tissue development; the CC terms cell projection, apical plasma, intracellular and cytoplasmic vesicle membrane, filopodium, lamellipodium, Golgi apparatus, nuclear chromatin, and cell leading edge; and the MF terms hormone and receptor binding, receptor, cytokine, and receptor ligand activity. The downregulated DEGs were enriched mainly in the BP terms biosynthetic and metabolic process, negative regulation of proteolysis and peptidase activity, and regulation of cytosolic calcium ion concentration; the CC terms inhibitor activity, ion binding, and cation binding; and the MF terms plasma membrane and presynapses, integral components of the plasma, intrinsic and reticulum membrane, presynapse, and dendrite.

The KEGG pathway enrichment analysis indicated that the upregulated DEGs were enriched mainly in the intestinal immune networks for IgA production, rheumatoid arthritis, cytokine–cytokine receptor interaction, and neuroactive ligand receptor interaction pathways. The downregulated DEGs were enriched mainly in the steroid biosynthesis pathway. The results of KEGG pathway enrichment analysis for the upregulated DEGs and downregulated DEGs are shown in Figure 6(a).

PPI network analysis

The PPI network was constructed using the STRING database to study interactions between the proteins encoded by the DEGs and to identify key potential key genes that may mediate the molecular mechanisms.

The PPI enrichment P value threshold was <0.01. A complex network of interactions was identified (Figure 7). The established PPI network consists of 39 nodes (genes encoding proteins) and 44 edges (interactions). The top 3 DEG-encoded proteins were actin alpha 2, smooth muscle (Acta2; degree = 9), calretinin (Calb2; degree = 8), and C-X-C motif chemokine ligand 12 (Cxcl12; degree = 8).

Biological validation by qPCR

To confirm the reliability of the data obtained using Illumina sequencing, we randomly selected six DEGs—three with upregulated expression (Hrct1, Il15, and Acta2) and three with downregulated expression (Calb2, Cbln4 and Moap1)—and assessed their expression by qPCR. The differences in the expression levels of these genes between the tMCAO group and the sham group were statistically significant. The differential expression trends of these genes revealed by qPCR were largely consistent with those revealed by RNA sequencing (Figure 6(b)).

Discussion

In this study, we demonstrated that microglial activation and WM damage were maintained in the hippocampus of tMCAO rats with cognitive impairment on day 28 after reperfusion. The mechanism of delayed poststroke damage and cognitive impairment may be related to the regulation of steroid biosynthesis, intestinal immunity, and long-term changes in gene expression patterns, including those of potential key genes such as Acta2, Calb2, and Cxcl12, in the hippocampus.

Almost 85% of stroke cases are associated with ischemic injury caused by MCAO.[19] Between 25% and 70% of ischemic stroke patients experience PSCI.[2] tMCAO is the most common procedure used to induce stroke in rodents. Compared with rats subjected to tMCAO for 60 min and 120 min, rats subjected to tMCAO for 90 min are more suitable for cognition-related behavioral testing studies.[20] The hippocampus plays essential roles in the processes of learning and memory and is vulnerable to ischemic injury. Ischemic hippocampal damage is associated with direct small and deep artery occlusion and indirect alterations in hippocampal–thalamic connections.[21,22] Delayed postischemic hippocampal damage could be essential in the development of cognitive impairment.

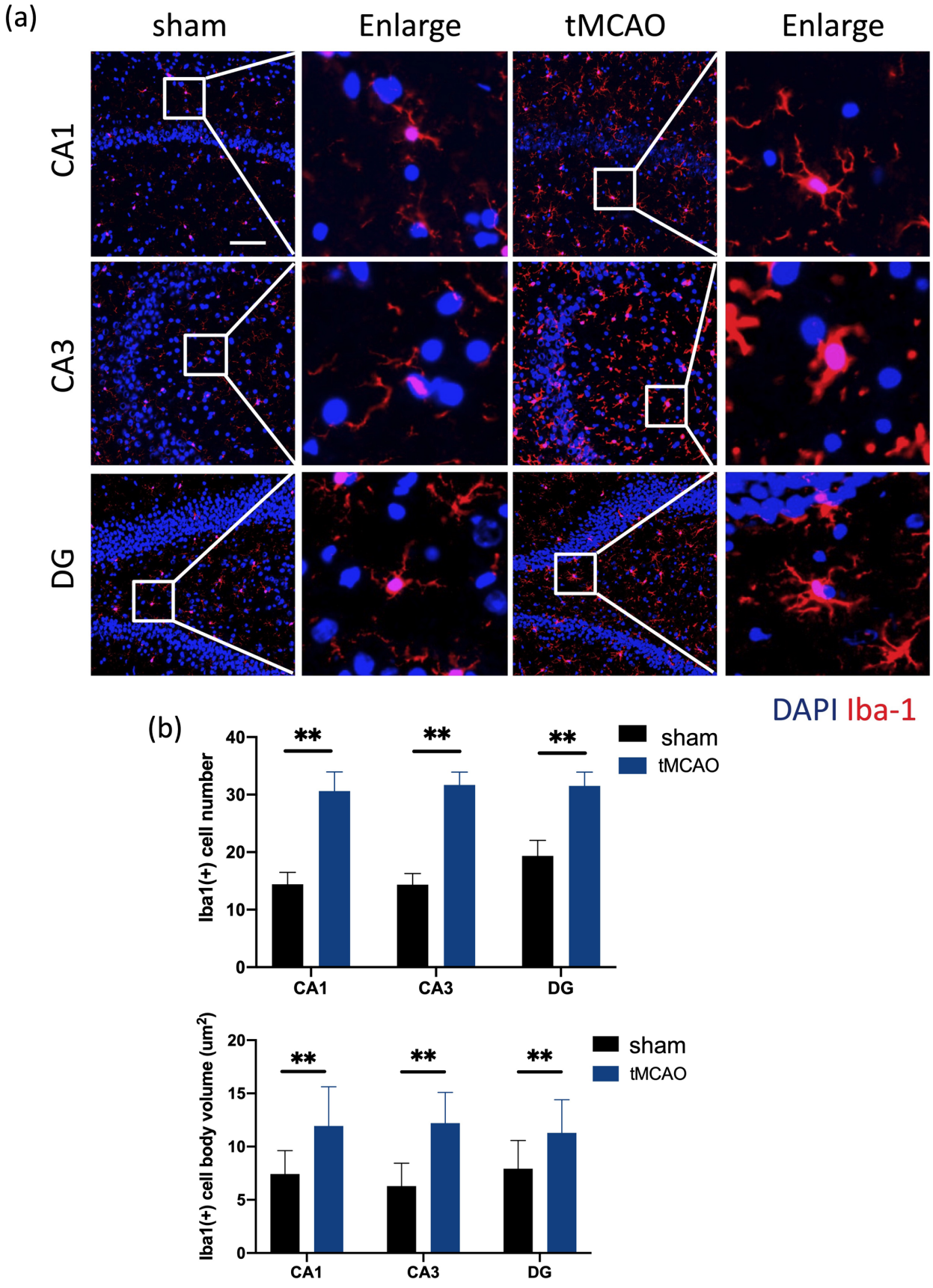

Figure 3. Assessment of microglial activation in the hippocampus. (a) Representative images of immunofluorescence staining for Iba-1 in the CA1 and CA3 regions and DG of the hippocampus. Bar = 50 μm. (b) Quantification of immunofluorescence staining for Iba-1 in the CA1 and CA3 regions and DG. tMCAO: transient middle cerebral artery occlusion.
*$P < 0.05$, **$P < 0.01$.

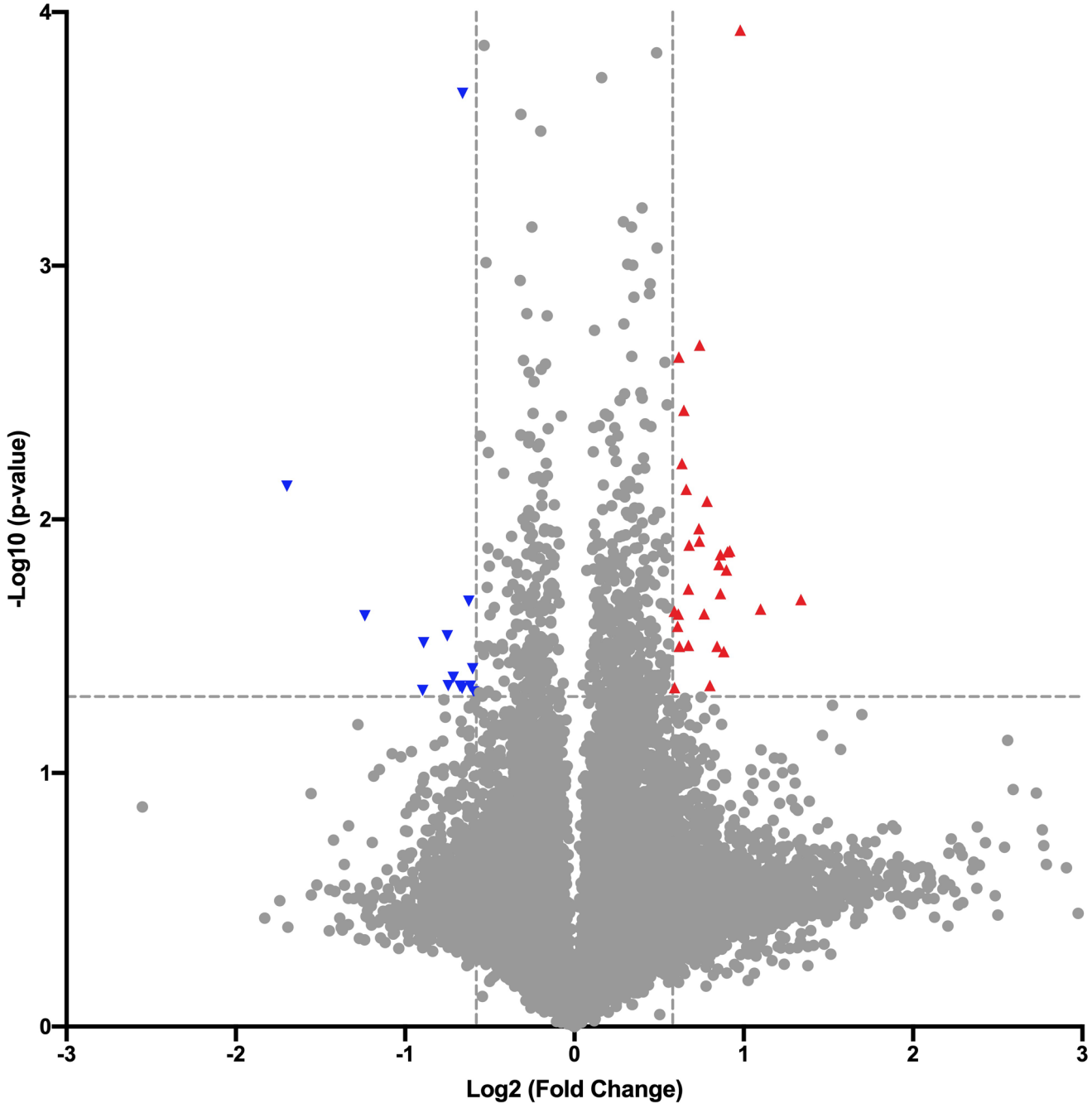

Figure 4. Volcano plot showing the DEGs. DEGs: differentially expressed genes.
The red and blue triangles represent genes with significantly upregulated and downregulated expression, respectively.

Neuroinflammation in the hippocampus can be maintained for long periods of time after stroke. Microglia were found to be rapidly activated, and their number continues to increase on day 7 after tMCAO and then gradually decrease over time. WM damage resulting from microglial activation is an important cause of PSCI. Consistent with previous findings, compared with sham-operated rats, tMCAO rats showed a decline in both learning ability and spatial memory on day 28 after reperfusion in this study. The number of activated microglial cells in the CA1 and CA3 regions and the DG of the hippocampus was significantly higher in the tMCAO group than in the sham group. WM damage described as disarrangement of nerve fibers, formation of vacuoles, and disappearance of myelinated fibers appeared in tMCAO rats on day 28 after reperfusion.

The molecular mechanisms of neuroinflammation in the hippocampus could involve long-term changes in gene expression patterns. Transcriptome analysis of the hippocampus carried out within the first 4.5–6 h and on day 1 after MCAO revealed associations of gene expression with various cellular and neurobiological events.[23] In contrast to previous studies, our study focused on the recovery stage of cerebral ischemia, during which cognitive impairment and neuroinflammation in the hippocampus are constantly

Table 2. Top 10 upregulated and downregulated DEGs (tMCAO group vs sham group).

Track ID	Gene name	Description	Fold change	*P* value
Upregulated DEGs				
ENSRNOG00000038905	AABR07048397.1	Sushi domain containing 1	2.528382887	0.020692293
ENSRNOG00000039336	Hrct1	Histidine rich carboxyl terminus 1	2.143519208	0.022596434
ENSRNOG00000003439	Il15	Interleukin-15	1.972390498	0.000117763
ENSRNOG00000025619	Ap1g2	Adaptor-related protein complex 1 subunit gamma 2	1.888159275	0.013322568
ENSRNOG00000058039	Acta2	Actin alpha 2, smooth muscle	1.873004795	0.013428274
ENSRNOG00000047218	Clic5	Chloride intracellular channel 5	1.862184666	0.015813153
ENSRNOG00000009922	Prlhr	Prolactin-releasing hormone receptor	1.842700694	0.033206695
ENSRNOG00000040213	AABR07014114.1	Unknown	1.817939059	0.013785466
ENSRNOG00000032232	Snrpg	Small nuclear ribonucleoprotein polypeptide G	1.817501345	0.019608009
ENSRNOG00000013589	Cxcl12	C-X-C motif chemokine ligand 12	1.806898424	0.015053969
Downregulated DEGs				
ENSRNOG00000016977	Calb2	Calbindin 2	0.308209988	0.007402119
ENSRNOG00000004372	Cbln4	Cerebellin 4 precursor protein	0.423909211	0.023973478
ENSRNOG00000016204	Lrrc24	Leucine-rich repeat containing 24	0.537511859	0.047315388
ENSRNOG00000033970	Moap1	Modulator of apoptosis 1	0.53950118	0.030678457
ENSRNOG00000023126	Rxfp3	Relaxin family peptide receptor 3	0.594495794	0.028770355
ENSRNOG00000021314	Fdft1	Farnesyl diphosphate farnesyl transferase 1	0.596624468	0.045229325
ENSRNOG00000029903	Spock3	SPARC/osteonectin, cwcv, and kazal-like domains proteoglycan 3	0.609171446	0.04195709
ENSRNOG00000036830	RGD1563200	Gametocyte specific factor 2	0.626005956	0.04547201
ENSRNOG00000060179	Gpc3	Glypican 3	0.631217456	0.04637843
ENSRNOG00000010268	Vom2r44	Vomeronasal 2 receptor 44	0.632772697	0.00020924

DEGs: differentially expressed genes; tMCAO: transient middle cerebral artery occlusion.

observed. The results of RNA sequencing in this study showed that the two pathways with the highest enrichment scores were steroid biosynthesis and intestinal immune network for IgA production. Classical steroid hormones, including estrogens, androgens, progestins, glucocorticoids, and mineralocorticoids, play critical roles in the regulation of reproduction and metabolism.[24] A study showed that MCAO rats could be predisposed to corticosterone-dependent distant neuroinflammatory hippocampal damage through the hypothalamic–pituitary–adrenal axis.[25] Treatment with progesterone was found to significantly attenuate microglial priming after stroke by modulating polarized microglia and the inflammatory environment in the hippocampus.[26]

The intestines are an important part of the immune system, and the gut microbiota is the main regulator of intestinal immune homoeostasis.[27] The gut microbiota is an important factor in the development of vascular cognitive impairment, which may affect the brain's cognitive functions through the brain–gut axis via neural, immune, endocrine, and metabolic pathways.[28,29] A fiber-deprived diet was reported to lead to cognitive impairment resulting from neuroinflammation in the hippocampus through altering the gut microbiota–hippocampus axis.[30] Atorvastatin-mediated improvement of intestinal barrier function and regulation of intestinal immunity were found to be involved in anti-inflammatory activity in stroke mice.[31] Thus, targeting the hypothalamic–pituitary–adrenal axis and gut microbiota–hippocampus axis could be fundamental new treatment directions for PSCI.

In addition, we performed PPI network analysis to detect interactions among the proteins encoded by the DEGs, and Acta2, Calb2, and Cxcl12 were identified as the top 3 DEG-encoded proteins. Acta2, also called alpha smooth muscle actin (α-SMA), is a prominent protein expressed on brain vessels that possibly influences blood vessel contraction.[32] A study reported increased levels of α-SMA, platelet endothelial cell adhesion molecule-1 (PECAM-1, also called CD31), and Iba-1 in the CA1 region of the hippocampus in Aβ1–42-injected mice on day 30 after injection.[33] Nicotinamide riboside reversed the angiotensin-induced decreases in the expression of α-SMA and the expression of neurofilament 200 (NF200) and myelin basic protein (MBP) in WM.[34] Calb2 was reported to be a modulator of neuronal excitability, including the induction of long-term potentiation and the basis of learning and memory.[35] Research has shown that a reduction in the Calb2 level negatively affects the cognitive activities of sporadic Alzheimer's disease model mice.[36] Granulocyte colony-stimulating factor (G-CSF) treatment was found to reverse cognitive impairment in Alzheimer's disease model mice by increasing the activation of resident microglia and increasing the numbers of calretinin-expressing cells in the hippocampus.[37] The chemokine Cxcl12 is widely expressed in neuronal and non-neuronal cells in the brain[38] and plays important roles in brain repair after ischemic stroke.[39] The immunomodulatory role of chemokines could reduce the destruction arising from the infiltration of inflammatory cells and consequent secondary damage after brain injury. Cxcl12 promotes neurite outgrowth on inhibitory myelin in cultured neurons and enhances the sprouting of axons after spinal cord injury.[40] Cxcl12 knockdown animals showed marked behavioral and learning deficits that were associated with impaired neurogenesis in the hippocampus.[41] These results not only indicate that these hub genes can be used as markers for PSCI during the stroke recovery period but also suggest that they may mediate the pathological process of PSCI.

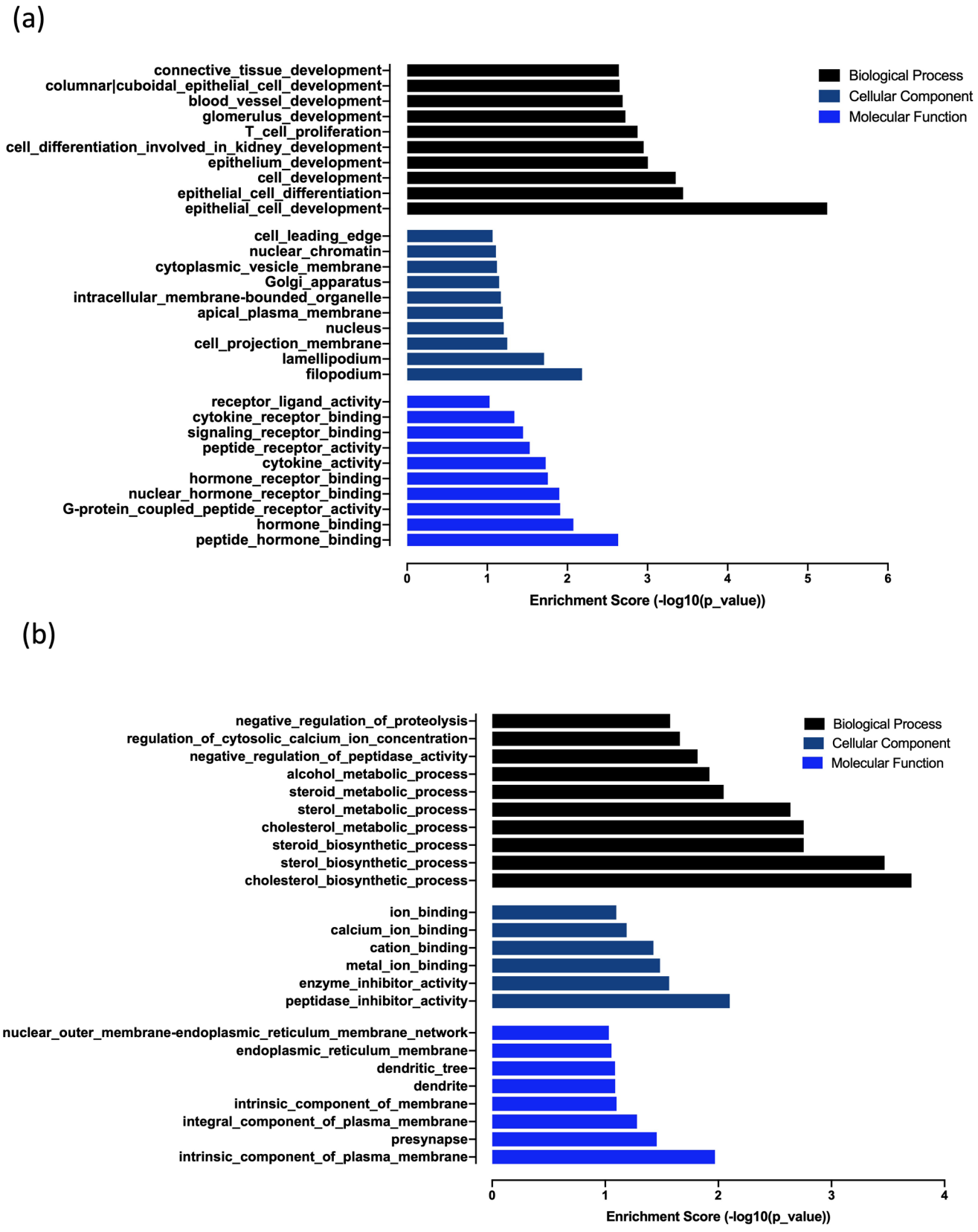

Figure 5. GO analysis of the DEGs in the two groups. (a) Bar plot showing the top 10 enrichment scores for BP, MF, and CC terms enriched with the upregulated DEGs. (b) Bar plot showing the top 10 enrichment scores for BP terms and all enrichment scores for MF and CC terms enriched with the downregulated DEGs. DEGs: differentially expressed genes; BP: biological process; MF: molecular function; CC: cellular component.

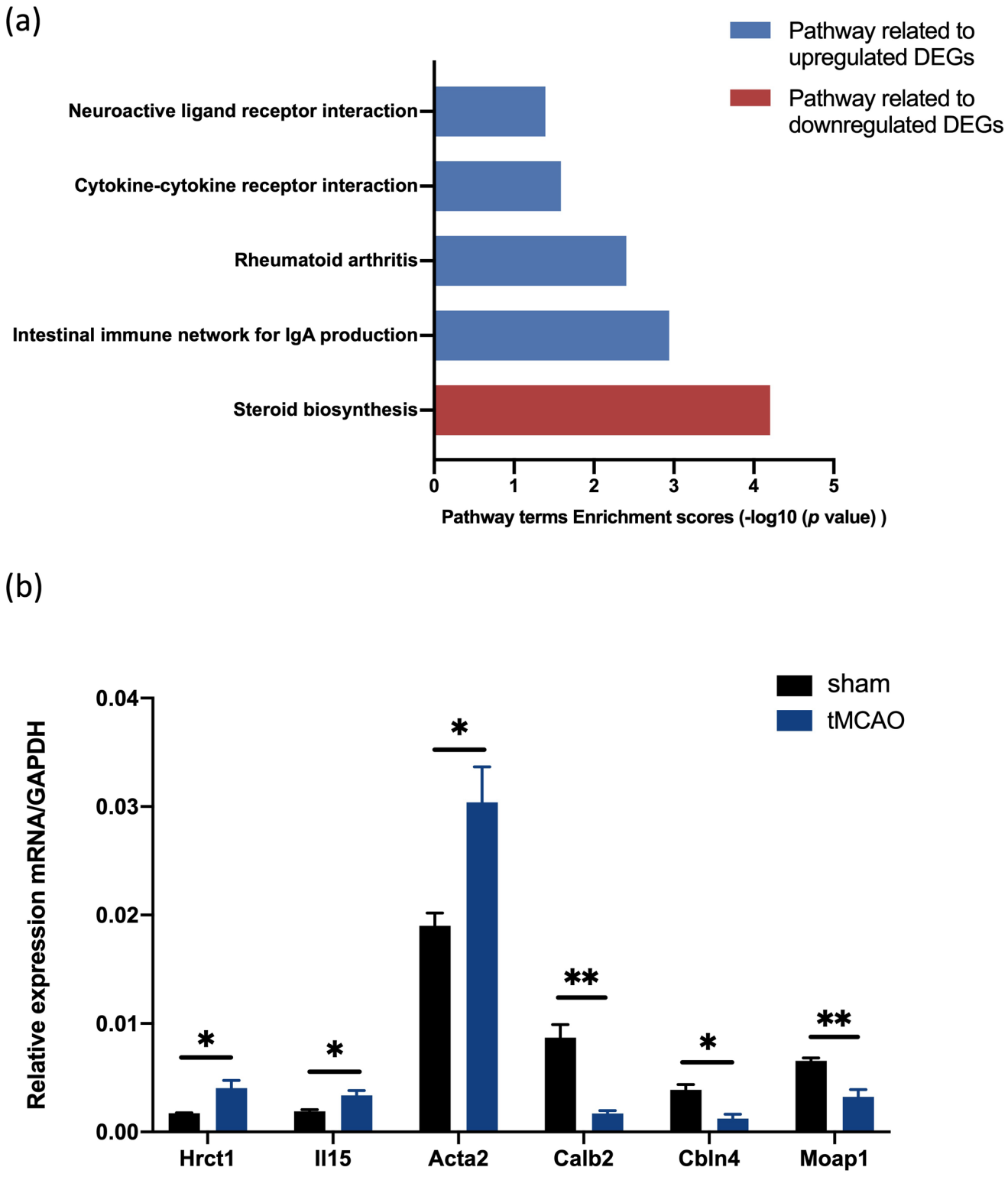

Figure 6. (a) KEGG analysis of the DEGs. Bar plot showing all significantly enriched pathways. (b) Validation of genes by qPCR. KEGG: Kyoto Encyclopedia of Genes and Genomes; DEGs: differentially expressed genes; qPCR: quantitative polymerase chain reaction; tMCAO: transient middle cerebral artery occlusion.
*$P < 0.05$, **$P < 0.01$.

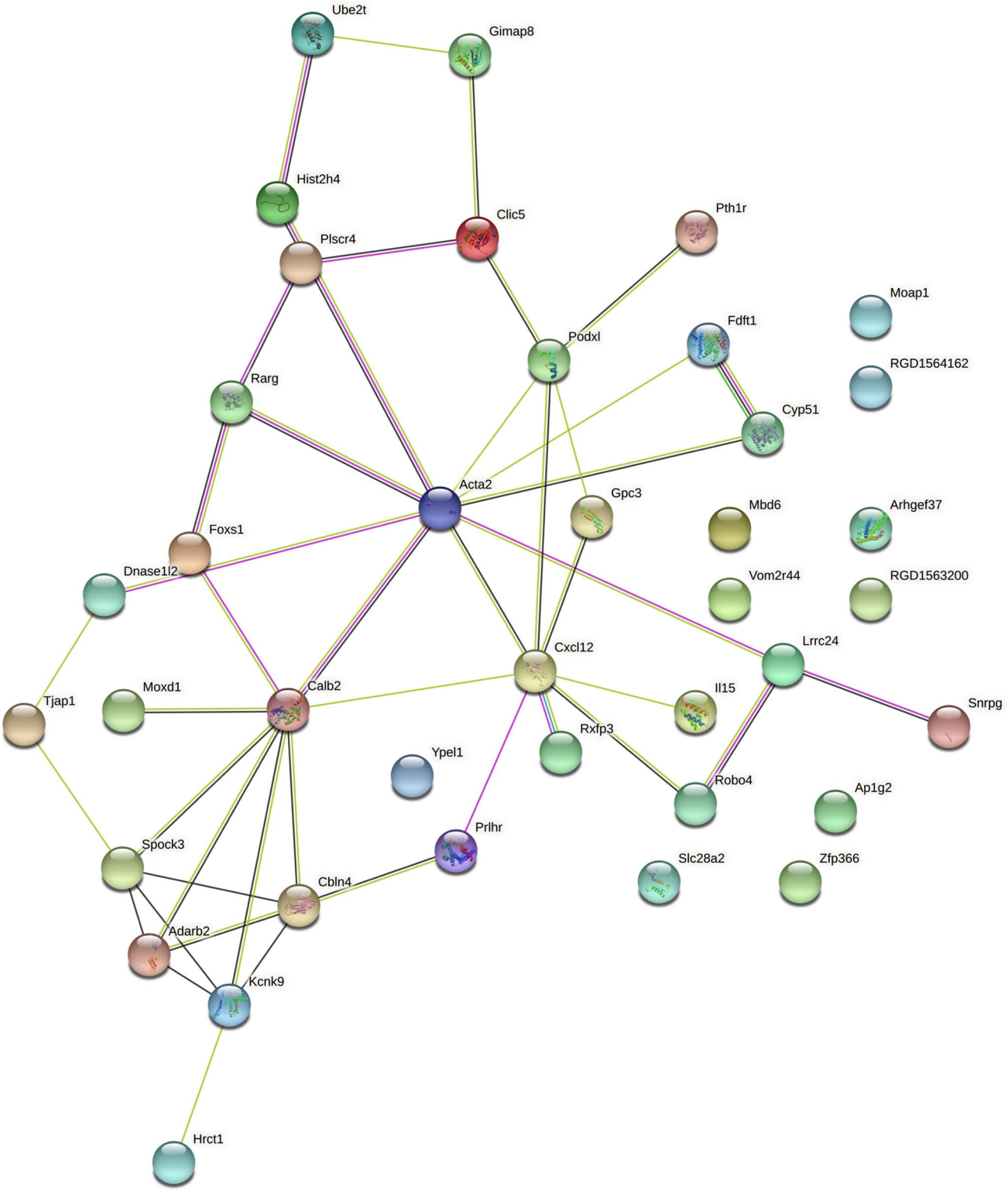

Figure 7. PPI network analysis of the DEGs. DEGs: differentially expressed genes.
The different line colors represent different sources of evidence for interactions: blue lines—data from curated databases, purple lines—experimentally determined data, green lines—text mining data, and black lines—coexpression data.

Conclusions

In summary, the results of this study indicate an important role of neuroinflammation in the development of PSCI and changes in the expression of regulatory genes in the hippocampus. This study may provide new insight into the pathogenesis and treatment of PSCI. However, in-depth experiments with large samples are needed to confirm these findings.

AUTHORS' CONTRIBUTIONS

JC and JH conceived and designed the study and prepared the manuscript. JC carried out the bioinformatic analyses. JH supervised the bioinformatic analyses. JC, JH, CL, YZ, and XZ performed animal experiments, qPCR, TTC staining, immunofluorescence staining, and LFB staining. MX and HW performed the statistical analyses. All authors participated in data analysis and approved the final version of this manuscript.

ACKNOWLEDGEMENTS

The study was conducted at the Guangdong Provincial Key Laboratory of Diagnosis and Treatment of Major Neurological Diseases, Guangdong Provincial Engineering Center for Major Neurological Disease Treatment, Guangdong Provincial Translational Medicine Innovation Platform for Diagnosis and Treatment of Major Neurological Disease, and Guangdong Provincial Clinical Research Center for Neurological Diseases. We thank Zubiao Song from The First Affiliated Hospital, Sun Yat-Sen University, for his technical assistance.

DECLARATION OF CONFLICTING INTERESTS

The author(s) declared no potential conflicts of interest with respect to the research, authorship, and/or publication of this article.

FUNDING

The author(s) disclosed receipt of the following financial support for the research, authorship, and/or publication of this article: This study was supported by the National Natural Science Foundation of China (grant numbers 81672259 and 81472156 to HW) and the Guangdong Basic and Applied Basic Research Foundation (grant numbers 2019A1515010388 to HW).

ORCID ID

Hongmei Wen https://orcid.org/0000-0002-0339-2498

REFERENCES

1. Wang W, Jiang B, Sun H, Ru X, Sun D, Wang L, Wang L, Jiang Y, Li Y, Wang Y, Chen Z, Wu S, Zhang Y, Wang D, Wang Y, Feigin VL, NESS-China Investigators. Prevalence, incidence, and mortality of stroke in China: results from a nationwide population-based survey of 480 687 adults. *Circulation* 2017;**135**:759–71
2. Chung C, Pollock A, Campbell T, Durward B, Hagen S. Cognitive rehabilitation for executive dysfunction in adults with stroke or other adult nonprogressive acquired brain damage. *Stroke* 2013;**44**:e77–18
3. Chander RJ, Lam BYK, Lin X, Ng AYT, Wong APL, Mok VCT, Kandiah N. Development and validation of a risk score (CHANGE) for cognitive impairment after ischemic stroke. *Sci Rep* 2017;**7**:12441
4. Ding MY, Xu Y, Wang YZ, Li PX, Mao YT, Yu JT, Cui M, Dong Q. Predictors of cognitive impairment after stroke: a prospective stroke cohort study. *J Alzheimers Dis* 2019;**71**:1139–51
5. Sivakumar L, Riaz P, Kate M, Jeerakathil T, Beaulieu C, Buck B, Camicioli R, Butcher K. White matter hyperintensity volume predicts persistent cognitive impairment in transient ischemic attack and minor stroke. *Int J Stroke* 2017;**12**:264–72
6. Thiel A, Cechetto DF, Heiss WD, Hachinski V, Whitehead SN. Amyloid burden, neuroinflammation, and links to cognitive decline after ischemic stroke. *Stroke* 2014;**45**:2825–9
7. Katzan IL, Thompson NR, Uchino K, Lapin B. The most affected health domains after ischemic stroke. *Neurology* 2018;**90**:e1364–71
8. Laakso HM, Hietanen M, Melkas S, Sibolt G, Curtze S, Virta M, Ylikoski R, Pohjasvaara T, Kaste M, Erkinjuntti T, Jokinen H. Executive function subdomains are associated with post-stroke functional outcome and permanent institutionalization. *Eur J Neurol* 2019;**26**:546–52
9. Lisman J, Buzsaki G, Eichenbaum H, Nadel L, Ranganath C, Redish AD. Viewpoints: how the hippocampus contributes to memory, navigation and cognition. *Nat Neurosci* 2017;**20**:1434–47
10. Shishkina GT, Kalinina TS, Gulyaeva NV, Lanshakov DA, Dygalo NN. Changes in gene expression and neuroinflammation in the hippocampus after focal brain ischemia: involvement in the long-term cognitive and mental disorders. *Biochemistry (Mosc)* 2021;**86**:657–66
11. Longa EZ, Weinstein PR, Carlson S, Cummins R. Reversible middle cerebral artery occlusion without craniectomy in rats. *Stroke* 1989;**20**:84–91
12. Niu RN, Shang XP, Teng JF. Overexpression of Egr2 and Egr4 protects rat brains against ischemic stroke by downregulating JNK signaling pathway. *Biochimie* 2018;**149**:62–70
13. Bederson JB, Pitts LH, Tsuji M, Nishimura MC, Davis RL, Bartkowski H. Rat middle cerebral artery occlusion: evaluation of the model and development of a neurologic examination. *Stroke* 1986;**17**:472–6
14. Bieber M, Gronewold J, Scharf AC, Schuhmann MK, Langhauser F, Hopp S, Mencl S, Geuss E, Leinweber J, Guthmann J, Doeppner TR, Kleinschnitz C, Stoll G, Kraft P, Hermann DM. Validity and reliability of neurological scores in mice exposed to middle cerebral artery occlusion. *Stroke* 2019;**50**:2875–82
15. Huang M, Xiao C, Zhang L, Li L, Luo J, Chen L, Hu X, Zheng H. Bioinformatic analysis of exosomal microRNAs of cerebrospinal fluid in ischemic stroke rats after physical exercise. *Neurochem Res* 2021;**46**:1540–53
16. Jiang T, Zhang L, Pan X, Zheng H, Chen X, Li L, Luo J, Hu X. Physical exercise improves cognitive function together with microglia phenotype modulation and remyelination in chronic cerebral hypoperfusion. *Front Cell Neurosci* 2017;**11**:404
17. Qin C, Fan WH, Liu Q, Shang K, Murugan M, Wu LJ, Wang W, Tian DS. Fingolimod protects against ischemic white matter damage by modulating microglia toward M2 polarization via STAT3 pathway. *Stroke* 2017;**48**:3336–46
18. Wakita H, Tomimoto H, Akiguchi I, Kimura J. Glial activation and white matter changes in the rat brain induced by chronic cerebral hypoperfusion: an immunohistochemical study. *Acta Neuropathol* 1994;**87**:484–92
19. Robinson RG, Jorge RE. Post-stroke depression: a review. *Am J Psychiatry* 2016;**173**:221–31
20. Sun J, Sun R, Li C, Luo X, Chen J, Hong J, Zeng Y, Wang QM, Wen H. NgR1 pathway expression in cerebral ischemic Sprague-Dawley rats with cognitive impairment. *Iran J Basic Med Sci* 2021;**24**:767–75
21. Baumgartner P, El Amki M, Bracko O, Luft AR, Wegener S. Sensorimotor stroke alters hippocampo-thalamic network activity. *Sci Rep* 2018;**8**:15770
22. El Amki M, Clavier T, Perzo N, Bernard R, Guichet PO, Castel H. Hypothalamic, thalamic and hippocampal lesions in the mouse MCAO model: potential involvement of deep cerebral arteries? *J Neurosci Methods* 2015;**254**:80–5
23. Chung JY, Yi JW, Kim SM, Lim YJ, Chung JH, Jo DJ. Changes in gene expression in the rat hippocampus after focal cerebral ischemia. *J Korean Neurosurg Soc* 2011;**50**:173–8
24. Stanisić V, Lonard DM, O'Malley BW. Modulation of steroid hormone receptor activity. *Prog Brain Res* 2010;**181**:153–76
25. Onufriev MV, Moiseeva YV, Zhanina MY, Lazareva NA, Gulyaeva NV. A comparative study of koizumi and longa methods of intraluminal filament middle cerebral artery occlusion in rats: early corticosterone and inflammatory response in the hippocampus and frontal cortex. *Int J Mol Sci* 2021;**22**:13544
26. Espinosa-Garcia C, Sayeed I, Yousuf S, Atif F, Sergeeva EG, Neigh GN, Stein DG. Stress primes microglial polarization after global ischemia: therapeutic potential of progesterone. *Brain Behav Immun* 2017;**66**:177–92
27. Mowat AM, Agace WW. Regional specialization within the intestinal immune system. *Nat Rev Immunol* 2014;**14**:667–85
28. Li S, Shao Y, Li K, HuangFu C, Wang W, Liu Z, Cai Z, Zhao B. Vascular cognitive impairment and the gut microbiota. *J Alzheimers Dis* 2018;**63**:1209–22

29. Welcome MO. Gut microbiota disorder, gut epithelial and blood-brain barrier dysfunctions in etiopathogenesis of dementia: molecular mechanisms and signaling pathways. *Neuromolecular Med* 2019;**21**:205–26
30. Shi H, Ge X, Ma X, Zheng M, Cui X, Pan W, Zheng P, Yang X, Zhang P, Hu M, Hu T, Tang R, Zheng K, Huang XF, Yu Y. A fiber-deprived diet causes cognitive impairment and hippocampal microglia-mediated synaptic loss through the gut microbiota and metabolites. *Microbiome* 2021;**9**:223
31. Zhang P, Zhang X, Huang Y, Chen J, Shang W, Shi G, Zhang L, Zhang C, Chen R. Atorvastatin alleviates microglia-mediated neuroinflammation via modulating the microbial composition and the intestinal barrier function in ischemic stroke mice. *Free Radic Biol Med* 2021;**162**:104–17
32. Yuan SM. alpha-smooth muscle actin and ACTA2 gene expressions in vasculopathies. *Braz J Cardiovasc Surg* 2015;**30**:644–9
33. Calvo-Flores Guzman B, Elizabeth Chaffey T, Hansika Palpagama T, Waters S, Boix J, Tate WP, Peppercorn K, Dragunow M, Waldvogel HJ, Faull RLM, Kwakowsky A. The interplay between beta-amyloid 1-42 (Abeta1-42)-induced hippocampal inflammatory response, p-tau, vascular pathology, and their synergistic contributions to neuronal death and behavioral deficits. *Front Mol Neurosci* 2020;**13**:522073
34. Li CC, Chen WX, Wang J, Xia M, Jia ZC, Guo C, Tang XQ, Li MX, Yin Y, Liu X, Feng H. Nicotinamide riboside rescues angiotensin II-induced cerebral small vessel disease in mice. *CNS Neurosci Ther* 2020;**26**:438–47
35. Camp AJ, Wijesinghe R. Calretinin: modulator of neuronal excitability. *Int J Biochem Cell Biol* 2009;**41**:2118–21
36. Coronas-Samano G, Baker KL, Tan WJ, Ivanova AV, Verhagen JV. Fus1 KO mouse as a model of oxidative stress-mediated sporadic Alzheimer's disease: circadian disruption and long-term spatial and olfactory memory impairments. *Front Aging Neurosci* 2016;**8**:268
37. Sanchez-Ramos J, Song S, Sava V, Catlow B, Lin X, Mori T, Cao C, Arendash GW. Granulocyte colony stimulating factor decreases brain amyloid burden and reverses cognitive impairment in Alzheimer's mice. *Neuroscience* 2009;**163**:55–72
38. Guyon A. CXCL12 chemokine and its receptors as major players in the interactions between immune and nervous systems. *Front Cell Neurosci* 2014;**8**:65
39. Zhang Y, Zhang H, Lin S, Chen X, Yao Y, Mao X, Shao B, Zhuge Q, Jin K. SDF-1/CXCR7 chemokine signaling is induced in the peri-infarct regions in patients with ischemic stroke. *Aging Dis* 2018;**9**:287–95
40. Jaerve A, Müller HW. Chemokines in CNS injury and repair. *Cell Tissue Res* 2012;**349**:229–48
41. Trousse F, Jemli A, Silhol M, Garrido E, Crouzier L, Naert G, Maurice T, Rossel M. Knockdown of the CXCL12/CXCR7 chemokine pathway results in learning deficits and neural progenitor maturation impairment in mice. *Brain Behav Immun* 2019;**80**:697–710

(Received May 9, 2022, Accepted January 13, 2023)